

Lakshmi Dharmarajan,^{a,b}
 Jessica L. Kraszewski,^{a,c}
 Biswarup Mukhopadhyay^{a,b,c,d,*}
 and Pete W. Dunten^{e*}

^aVirginia Bioinformatics Institute, USA,

^bGenetics, Bioinformatics and Computational Biology PhD Program, Virginia Polytechnic Institute and State University, Blacksburg, Virginia 24061, USA, ^cDepartment of Biochemistry, Virginia Polytechnic Institute and State University, Blacksburg, Virginia 24061, USA, ^dDepartment of Biological Sciences, Virginia Polytechnic Institute and State University, Blacksburg, Virginia 24061, USA, and ^eStanford Synchrotron Radiation Lightsource, Stanford University, Menlo Park, California 94025, USA

Correspondence e-mail: biswarup@vt.edu,
 pete@slac.stanford.edu

Received 22 August 2009

Accepted 16 October 2009

Expression, purification and crystallization of an archaeal-type phosphoenolpyruvate carboxylase

An archaeal-type phosphoenolpyruvate carboxylase (PepcA) from *Clostridium perfringens* has been expressed in *Escherichia coli* in a soluble form with an amino-terminal His tag. The recombinant protein is enzymatically active and two crystal forms have been obtained. Complete diffraction data extending to 3.13 Å resolution have been measured from a crystal soaked in KAu(CN)₂, using radiation at a wavelength just above the Au L_{III} edge. The asymmetric unit contains two tetramers of PepcA.

1. Introduction

Phosphoenolpyruvate carboxylase (Pepc) catalyzes the formation of oxaloacetate (OAA) from phosphoenolpyruvate (PEP) and bicarbonate. The enzyme from C₄ plants has been intensively studied as it plays a vital role in CO₂ fixation (Izui *et al.*, 2004; Chollet *et al.*, 1996). The C₄ compounds produced after carboxylation of PEP are transported into chloroplasts, where subsequent decarboxylation supplies ribulose 1,5-bisphosphate carboxylase/oxygenase (RuBisCO) with a high local concentration of CO₂ (Raines, 2006). C₄ plants are thus able to suppress oxygenation, a competing reaction catalyzed by RuBisCO that lowers the efficiency of CO₂ fixation (Raines, 2006). C₃ plants lack a mechanism to concentrate CO₂ and fix CO₂ with only ~50% efficiency (Häusler *et al.*, 2002). Attempts to express C₄-type Pepc in C₃ plants have not improved the efficiency of carbon fixation (Häusler *et al.*, 2002). The high K_m of the introduced C₄-type Pepc for PEP and its sensitivity to inhibition by malate are thought to be responsible (Fukayama *et al.*, 2003; Endo *et al.*, 2008). The activity of Pepc in plants is modulated by both positive and negative allosteric regulation *via* binding of small-molecule effectors and by phosphorylation (Izui *et al.*, 2004). The *Escherichia coli* enzyme has also been studied in detail (Izui *et al.*, 2004). The bacterial enzyme is highly homologous to the plant enzyme (Izui *et al.*, 2004) and subject to allosteric regulation, although not *via* phosphorylation (Izui *et al.*, 2004). The archaeal-type Pepc (PepcA), in contrast, shows a simpler pattern of regulation (Patel *et al.*, 2004; Ettema *et al.*, 2004; Sako *et al.*, 1996, 1997). No inhibitors or activators are known for PepcA from *Methanothermobacter sociabilis* or *Methanothermobacter thermautotrophicus* (Matsumura *et al.*, 2006). PepcA is therefore an interesting candidate for expression in C₃ plants with the goal of improving the efficiency of carbon fixation.

PepcA and Pepc share only 12–16% sequence identity and the only X-ray structures available are those of Pepc from *E. coli* and maize (Kai *et al.*, 1999; Matsumura *et al.*, 2002). The enzymes from *E. coli* and maize are homotetramers of 4 × 883 and 4 × 970 residues, respectively. In solution, both dimers and tetramers of *E. coli* Pepc are present, with a shift towards the tetrameric form in the presence of the allosteric inhibitor aspartate (Coomes *et al.*, 1985). The PepcAs from *Methanothermobacter sociabilis*, *Sulfolobus acidocaldarius* and *Methanothermobacter thermautotrophicus* have all been reported to be tetramers in solution based on gel filtration (Sako *et al.*, 1996, 1997; Patel *et al.*, 2004). Attempts have been made to model the structure of PepcA based on the known X-ray structures of *E. coli* and maize



© 2009 International Union of Crystallography
 All rights reserved

Pepcs (Matsumura *et al.*, 2006). The PepcA structure has also been targeted by structural genomics consortia, given the difficulty of modeling the fold. The PepcA-sequence family includes many representatives from the archaea and three bacterial homologs that are found in *Clostridium perfringens*, *Oenococcus oeni* and *Leuconostoc mesenteroides* (Patel *et al.*, 2004). The sequence most closely related to that of PepcA from *C. perfringens* is from an archaeal methanogen, *Methanopyrus kandleri*; the sequences are 537 and 532 residues in length, respectively, and share 35% sequence identity. Production of the archaeal enzymes in *E. coli* has been difficult (Ettema *et al.*, 2004; Kraszewski & Mukhopadhyay, 2005). The 537-residue PepcA homolog from the bacterium *C. perfringens* expressed well in *E. coli* when fused to an N-terminal His₁₀ tag. Crystals of the recombinant tagged protein diffracted to ~3 Å resolution and complete X-ray data have been collected.

2. Materials and methods

2.1. Cloning and protein expression

The ORF CPE1094 was PCR-amplified from *C. perfringens* strain 13 chromosomal DNA using the oligonucleotides CpePpc/1F, 5'-GAAAAGGGGGACTTCATATGAAGATACCTTGTTCCATGATGAC-3' and CpePpc/2R, 5'-CAAGGATCCTTTAGCCTATACCTTCTTACTTTACCCATTC-3'. The amplified DNA was digested with *Nde*I and *Bam*HI and cloned into similarly digested pET19b (Novagen, San Diego, California, USA). In the resulting construct, the full-length PepcA protein is preceded by the affinity tag MGH-HHHHHHHHHSSGHIDDDDKH. The PepcA expression plasmid, designated pJLK15-19b, was introduced into *E. coli* strain BL21 (DE3) (pRIL). Cultures were grown at 310 K in LB medium containing ampicillin (100 µg ml⁻¹) and chloramphenicol (25 µg ml⁻¹) to an optical density of 0.5 before adding IPTG (1 mM) to induce expression of PepcA. Cells were harvested 4 h post-induction by centrifugation for 10 min at 9600g and the cell pellets were stored at 253 K.

2.2. Protein purification

5 g of cell pellet was thawed on ice with 10 ml 100 mM potassium phosphate buffer pH 7.0. Cells were broken by passage through a French pressure cell. 0.02 g DNase was added and the mixture was incubated on ice for 20 min. The extract was centrifuged at 18 000g for 1 h at 277 K. All further purification steps were carried out at 293 K. The soluble portion of the extract was brought to final concentrations of 50 mM potassium phosphate pH 7.0, 300 mM NaCl and 10 mM imidazole (equilibration buffer). The extract was filtered through a 0.2 µm filter and loaded onto a 10 ml Superflow Ni²⁺-NTA column (Qiagen Inc., Valencia, California, USA) at a flow rate of 1 ml min⁻¹. The column was washed with four column volumes of equilibration buffer and then with two volumes of a solution containing 50 mM potassium phosphate buffer pH 7, 10 mM imidazole, 400 mM NaCl. Washing was continued with equilibration buffer until the absorption at 280 nm was stable. PepcA was eluted using an imidazole gradient over six column volumes (50–600 mM imidazole in equilibration buffer). Column fractions were analyzed using SDS-PAGE. The 400–500 mM imidazole fractions contained homogenous PepcA. The buffer was exchanged *via* ultrafiltration to 50 mM sodium phosphate pH 7, 150 mM NaCl (SEC buffer) and the protein was concentrated to a volume of 2 ml. The Ni²⁺-NTA pool was loaded onto a HiPrep 16/60 Sephacryl S-300 HR column pre-equilibrated with SEC buffer. PepcA was eluted using the same buffer. The protein was concentrated to 5 mg ml⁻¹ (determined using the Brad-

ford Coomassie-binding assay; Bio-Rad, Hercules, California, USA) and the buffer was changed to 20 mM HEPES pH 7 *via* ultrafiltration prior to crystallization.

The enzyme activity was assayed as described previously (Patel *et al.*, 2004) but with a modified assay mixture containing 50 mM HEPES pH 7.2, 0.2 mM NADH, 30 mM KHCO₃, 1.5 mM Na PEP, 2 mM MgCl₂ and 1 U ml⁻¹ thermophilic malate dehydrogenase from *Thermus flavus* (Sigma, St Louis, Missouri, USA).

2.3. Crystallization and data collection

Crystals were grown *via* hanging-drop vapor diffusion at 295 K in drops formed from 2 µl protein solution plus 2 µl reservoir solution. Hexagonal rods appeared within 1–3 d using 0.2–0.3 M magnesium formate, 0.1 M bis-Tris pH 5.5 or 0.1 M Tris pH 8.5 as precipitant. These crystals diffracted to only 8 Å after cryoprotection with either 20% PEG 200 or ethylene glycol. Blocks appeared after 6 d using 1.25–1.5 M sodium malonate pH 7 as precipitant. These crystals could be cryoprotected with 1.5 M sodium malonate pH 7 and diffracted to 3 Å resolution. A native data set was collected at 100 K from a crystal of approximate dimensions 0.15 × 0.2 × 0.4 mm using a Rayonix MX-325 detector on SSRL BL9-2. Data collection was based on a strategy suggested by *Web-Ice* (González *et al.*, 2008). 450 images were collected with a Δφ of 0.4° to give a total of 180° of data. The *a** axis was closest to the rotation axis. Data integration and scaling were performed with *MOSFLM* (Leslie, 1992) and *SCALA* (Evans, 1997). A derivative was prepared by soaking a crystal in 1.5 M sodium malonate pH 7, 2 mM KAu(CN)₂ for 16 h. A SAD data set was collected at 100 K from a soaked crystal of approximate dimensions 0.1 × 0.1 × 0.2 mm using a Rayonix MX-325 detector on SSRL BL11-1. 480 images were collected with a Δφ of 0.75° to give a total of 360° of data. The *c** axis was closest to the rotation axis, minimizing the problem of overlapped reflections. Data integration and scaling were performed with *HKL-2000* (Otwinowski & Minor, 1997), keeping *I*⁺ and *I*⁻ separate during scaling and calculation of *R*_{merge}. For both data sets, the total X-ray dose was estimated before choosing the exposure time per image to avoid radiation damage to the crystals. The dose estimated by *RADDOSE* (Paithankar *et al.*, 2009) was 2.4 MGy for the native data set and 2.5 MGy for the KAu(CN)₂-derivative data set.

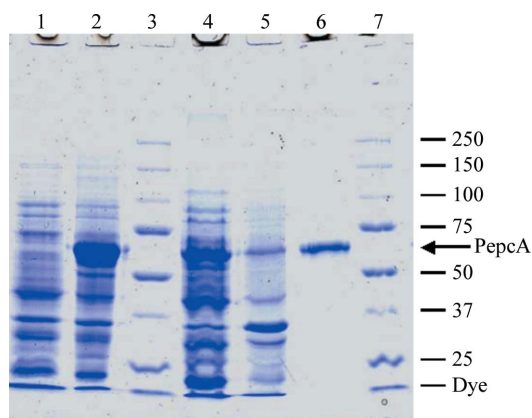


Figure 1
Purification of overexpressed PepcA. Lane 1, whole cell extract before induction of PepcA expression; lane 2, whole cell extract after IPTG induction; lane 3, molecular-weight markers; lane 4, soluble portion of the extract; lane 5, insoluble portion of the extract; lane 6, purified PepcA; lane 7, molecular-weight markers with mass indicated in kDa. The calculated molecular weight of His₁₀-tagged PepcA is 62.3 kDa.

Table 1

Data-collection statistics.

Values in parentheses are for the highest resolution shell.

	Native	KAu(CN) ₂
Beamline	SSRL BL9-2	SSRL BL11-1
Wavelength (Å)	0.97946	1.03948
Space group	<i>P</i> 2 ₁ 2 ₁ 2 ₁	<i>P</i> 2 ₁ 2 ₁ 2 ₁
Unit-cell parameters (Å)	<i>a</i> = 123.3, <i>b</i> = 164.1, <i>c</i> = 283.3	<i>a</i> = 121.4, <i>b</i> = 161.7, <i>c</i> = 280.1
Monomers per ASU	8	8
Matthews coefficient (Å ³ Da ⁻¹)	2.9	2.9
Resolution (Å)	3.13 (3.21–3.13)	3.13 (3.24–3.13)
Completeness (%)	82.6 (73.0)	100 (100)
Multiplicity	5.6 (5.5)	7.9 (7.8)
Unique reflections	84213	97165
<i>I</i> /σ(<i>I</i>)	7.1 (2.8)	23.4 (4.4)
<i>R</i> _{merge} †	0.165 (0.739)	0.098 (0.526)
Wilson <i>B</i> value (Å ²)	72	70

† $R_{\text{merge}} = \frac{\sum_{hkl} \sum_i |I_i(hkl) - \langle I(hkl) \rangle|}{\sum_{hkl} \sum_i I_i(hkl)}$, where $\langle I(hkl) \rangle$ is the mean intensity over all symmetry-related and equivalent reflections for reflection hkl and the $I_i(hkl)$ are the observed intensities for reflection hkl .

3. Results

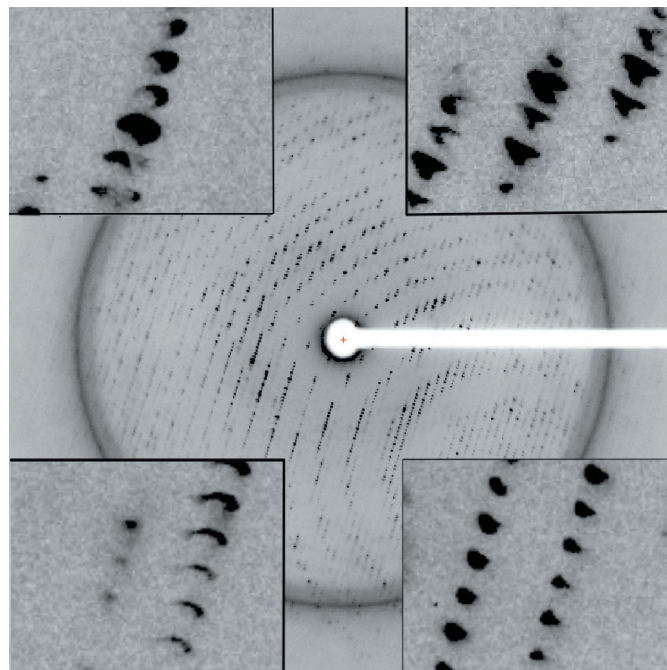
PepcA from *C. perfringens* with an N-terminal His₁₀ tag yielded soluble catalytically active protein. After Ni²⁺-affinity-based chromatography, the PepcA preparation was homogeneous as judged by denaturing SDS-PAGE (Fig. 1). The enzyme was further purified *via* gel filtration to remove aggregates. The apparent molecular weight of the enzyme based on the gel-filtration elution volume was 130 kDa, consistent with a dimer of 62.3 kDa subunits. The yield was 1.5 mg pure PepcA per gram of cell paste. The specific activity of the purified enzyme was typically in the range 38–65 μmol min⁻¹ mg⁻¹.

Crystals were obtained in the orthorhombic space group *P*2₁2₁2₁ using sodium malonate as a precipitant (Fig. 2). The unit-cell parameters of *a* = 123.3, *b* = 164.1, *c* = 283.3 Å suggested eight copies of PepcA per asymmetric unit, with a solvent content of 57% and a Matthews coefficient of 2.9 Å³ Da⁻¹. A slightly smaller unit cell was obtained for a crystal soaked in KAu(CN)₂, with *a* = 121.4, *b* = 161.7, *c* = 280.1 Å. Data with a useful anomalous signal were collected from the Au-containing crystal at a wavelength just above the Au *L*_{III} edge (Table 1). Two factors that contribute to the higher quality of the data from the Au-soaked crystal are the greater redundancy and the favorable orientation of the crystal (the longest axis was closest to the rotation axis). An additional feature unique to the native diffraction pattern was a variation in spot shape. In the native diffraction pattern the spot shape varied markedly across the face of the detector (Fig. 3*a*), whereas in the diffraction pattern of the KAu(CN)₂-soaked crystal the spot shape was uniform across the detector (Fig. 3*b*). Molecular replacement with models including the conserved Pepc

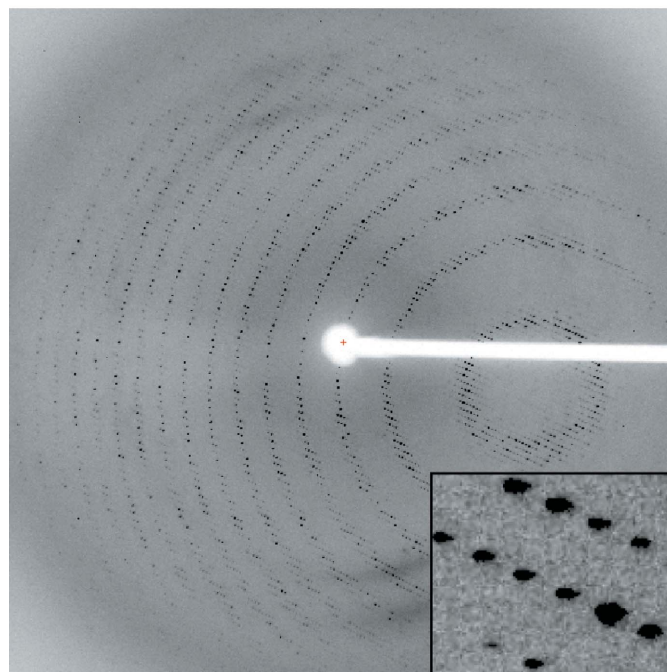

Figure 2

Crystals of PepcA grown in 1.5 M sodium malonate pH 7 together with 'haystacks' of needles and precipitate.

β-barrel was not successful. A SAD solution of the structure is under way. 16 gold sites were located with *SHELXD* and after density modification *SHELXE* reported a mean figure of merit of 0.459 (Sheldrick, 2008). The local symmetry of the gold sites indicates that the asymmetric unit contains two tetramers of PepcA and that the tetramers possess 222 point-group symmetry. The regulation of PepcA from *C. perfringens* has not been studied and it is not known what factors influence the quaternary structure of the enzyme. The



(a)



(b)

Figure 3

Diffraction patterns taken from PepcA crystals. (a) An 0.4° oscillation from the native data set, with insets in the image showing the variation of spot shape across the detector. The resolution at the detector edge was 3 Å. (b) An 0.75° oscillation from the KAu(CN)₂-soaked crystal. The resolution at the detector edge was 3.13 Å.

precipitant, malonate, may have favored the crystallization of tetramers. Malonate is an inhibitor of *E. coli* Peps and the quaternary structure of *E. coli* Peps is known to be sensitive to inhibitor binding (Corwin & Fanning, 1968; Coomes *et al.*, 1985). Whether or not the PepsA quaternary structure is also influenced by inhibitor binding is an open question.

C. perfringens strain 13 chromosomal DNA was a gift from Stephen Melville of the Department of Biological Sciences, Virginia Polytechnic Institute and State University. We thank Eric Johnson for help in protein purification. Portions of this research were carried out at the Stanford Synchrotron Radiation Lightsource, a national user facility operated by Stanford University on behalf of the US Department of Energy, Office of Basic Energy Sciences. The SSRL Structural Molecular Biology Program is supported by the Department of Energy, Office of Biological and Environmental Research and by the National Institutes of Health, National Center for Research Resources, Biomedical Technology Program and the National Institute of General Medical Sciences. The projects described were partially supported by Grant No. 5 P41 RR001209 from the National Center for Research Resources (NCRR), a component of the National Institutes of Health (NIH), and their contents are solely the responsibility of the authors and do not necessarily represent the official view of NCRR or NIH. LD received a graduate fellowship (2005) from the Virginia Tech Genetics, Bioinformatics and Computational Biology PhD program.

References

- Chollet, R., Vidal, J. & O'Leary, M. H. (1996). *Annu. Rev. Plant Physiol. Plant Mol. Biol.* **47**, 273–298.
- Coomes, M. W., Mitchell, B. K., Beezley, A. & Smith, T. E. (1985). *J. Bacteriol.* **164**, 646–652.
- Corwin, L. M. & Fanning, G. R. (1968). *J. Biol. Chem.* **243**, 3517–3525.
- Endo, T., Mihara, Y., Furumoto, T., Matsumura, H., Kai, Y. & Izui, K. (2008). *J. Exp. Bot.* **59**, 1811–1818.
- Ettema, T. J., Makarova, K. S., Jellema, G. L., Gierman, H. J., Koonin, E. V., Huynen, M. A., de Vos, W. M. & van der Oost, J. (2004). *J. Bacteriol.* **186**, 7754–7762.
- Evans, P. R. (1997). *Jnt CCP4/ESF-EACBM Newsl. Protein Crystallogr.* **33**, 22–24.
- Fukayama, H., Hatch, M. D., Tamai, T., Tsuchida, H., Sudoh, S., Furbank, R. T. & Miyao, M. (2003). *Photosynth. Res.* **77**, 227–239.
- González, A., Moorhead, P., McPhillips, S. E., Song, J., Sharp, K., Taylor, J. R., Adams, P. D., Sauter, N. K. & Soltis, S. M. (2008). *J. Appl. Cryst.* **41**, 176–184.
- Häusler, R. E., Hirsch, H. J., Kreuzaler, F. & Peterhansel, C. (2002). *J. Exp. Bot.* **53**, 591–607.
- Izui, K., Matsumura, H., Furumoto, T. & Kai, Y. (2004). *Annu. Rev. Plant Physiol. Plant Mol. Biol.* **55**, 69–84.
- Kai, Y., Matsumura, H., Inoue, T., Terada, K., Yoshinaga, T., Kihara, A., Tsumura, K. & Izui, K. (1999). *Proc. Natl Acad. Sci. USA*, **96**, 823–828.
- Kraszewski, J. L. & Mukhopadhyay, B. (2005). Unpublished work.
- Leslie, A. G. W. (1992). *Jnt CCP4/ESF-EACBM Newsl. Protein Crystallogr.* **26**.
- Matsumura, H., Izui, K. & Mizuguchi, K. (2006). *Protein Eng.* **19**, 409–419.
- Matsumura, H., Xie, Y., Shirakata, S., Inoue, T., Yoshinaga, T., Ueno, Y., Izui, K. & Kai, Y. (2002). *Structure*, **10**, 1721–1730.
- Otwinowski, Z. & Minor, W. (1997). *Methods Enzymol.* **276**, 307–326.
- Paithankar, K. S., Owen, R. L. & Garman, E. F. (2009). *J. Synchrotron Rad.* **16**, 152–162.
- Patel, H. M., Kraszewski, J. L. & Mukhopadhyay, B. (2004). *J. Bacteriol.* **186**, 5129–5137.
- Raines, C. A. (2006). *Plant Cell Environ.* **29**, 331–339.
- Sako, Y., Takai, K., Nishizaka, T. & Ishida, Y. (1997). *FEMS Microbiol. Lett.* **153**, 159–165.
- Sako, Y., Takai, K., Uchida, A. & Ishida, Y. (1996). *FEBS Lett.* **392**, 148–152.
- Sheldrick, G. M. (2008). *Acta Cryst.* **A64**, 112–122.